I&EC research
Industrial & Engineering Chemistry Research

Article

Cite This: Ind. Eng. Chem. Res. 2019, 58, 19702−19708

pubs.acs.org/IECR

Adsorption of Gases on Zeolitic Imidazolate Frameworks: Modeling with Equations of State for Confined Fluids and Pore Size Distribution Estimation

Gabriel D. Barbosa,*[,†] Leonardo Travalloni,[‡] Frederico W. Tavares,[†,‡] and Marcelo Castier[§]

[†]Programa de Engenharia Química, COPPE, Universidade Federal do Rio de Janeiro, Rio de Janeiro, C.P. 68542, Brazil
[‡]Escola de Química, Universidade Federal do Rio de Janeiro, Rio de Janeiro, C.P. 68542, Brazil
[§]Chemical Engineering Program, Texas A&M University at Qatar, Doha, P.O. Box 23874, Qatar

ABSTRACT: Certain gas separations, as that of propene from propane, are difficult and costly via methods such as distillation, conventionally used in oil and gas industries. Membrane-based separations using metal organic frameworks (MOFs) and, in particular, zeolitic imidazolate frameworks (ZIFs) are potential candidates for less expensive and more energy-efficient processes. Two effects define the performance of a given separation: diffusion and adsorption equilibrium. This works focuses on the latter: the adsorption equilibrium of gases on ZIFs has been correlated and predicted using an equation of state for confined fluids, which extends the Peng−Robinson model, widely used for process design in the oil and gas industries. Excellent agreement between experimental and calculated adsorption isotherms is obtained. In addition, we fitted pore size distributions (PSDs), under the initial assumption that these PSDs might present multiple peaks. In all cases, the fitted PSDs presented a single, narrow peak, which is consistent with the well-defined pore structure of the investigated ZIFs.

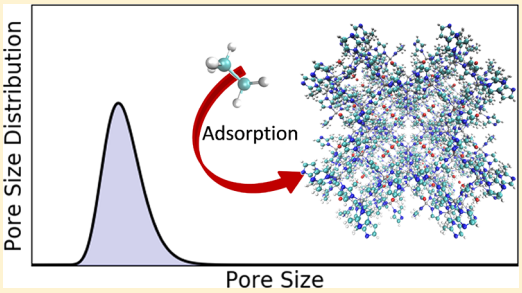

INTRODUCTION

Metal organic frameworks (MOFs) potentially enable the development of tailor-made membranes for specific separations by the selection of metals and ligands. There has been extensive experimental and modeling work on MOFs and, in particular, on zeolitic imidazolate frameworks (ZIFs), which comprise a class of MOFs. Recent results on the use of ZIFs show that they can be highly selective for certain gas separations,[1−9] especially of light hydrocarbons, which may otherwise be costly via methods conventionally used in industry, such as distillation. For many separations on ZIFs, there is evidence that diffusion,[10,11] rather than adsorption equilibrium, is the main mechanism for selectivity. Nonetheless, being able to predict adsorption equilibrium is an important objective because it informs about the limiting conditions for the operation of such separation processes.

Composed by tetrahedral metal aggregates and imidazolate linkers, the flexible structure, and chemical and thermal stability have been regarded as advantageous characteristics of ZIFs in separation processes.[12] In particular, the gate-opening effect, due to external stimuli on the adsorption behavior of gases (such as temperature and pressure conditions and adsorbate presence), is widely reported in the literature. The gate-opening effect on the separation of light alkanes and alkenes on ZIF-7 can be inferred from theoretical and experimental data.[13,14] In addition, the framework flexibility of ZIF-8 was verified through experimental and simulation data.[15−17]

There are several techniques to model adsorption equilibrium, which vary widely in level of detail and computational effort. Monte Carlo (MC) and molecular dynamics (MD) simulations of fluids in ZIFs account for the interactions of the atoms of the fluid and of the ZIF, which can either be considered as rigid or flexible. Both MC and MD require large computational effort and, despite the amount of information they provide, it is currently unfeasible to use them in most chemical process design calculations. Both classical density functional theory[18,19] and simplified local density theory[20,21] are alternative approaches with smaller computational requirements, which however may still be excessive for practical chemical process design.

For process design, it is often sufficient to correlate and predict adsorbed amounts as a function of the bulk fluid composition and pressure, as in an adsorption isotherm. To this end, several equations of state have been developed in recent years. The usual approach is to start from an equation of state (EOS) originally for bulk fluids and include contributions related to the interactions between the fluid molecules and the confining wall. The original EOS for these extensions can be either cubic in volume[22−30] or not.[31,32] The shape of the confining wall affects the results, and it is usual to develop models for void spaces with well-defined and simple geo-

Received: September 18, 2019
Accepted: October 3, 2019
Published: October 3, 2019

DOI: 10.1021/acs.iecr.9b05221
Ind. Eng. Chem. Res. 2019, 58, 19702−19708

metries, such as slit, cylindrical, and spherical pores. In particular, the attractive feature of the models proposed by Travalloni et al.[25−27] and Barbosa et al.[29,30,33] is that they tend to the originating EOS when the pore size increases. In this way, the same EOS can be used to model the bulk and the confined fluid. Formulating an adsorption equilibrium calculation for a heterogeneous solid is simple with this approach: all it takes is to consider the existence of multiple pore types, each of them characterized by its size and interaction energy. Another attractive feature of such models is that their computational load is similar to that of the original EOS, which renders them practical for process design.

The goal of this work is to model the adsorption equilibrium of gases on ZIFs using extended forms of the Peng−Robinson EOS[34] for confined fluids in spherical pores. In addition, we fit pore size distributions (PSDs) in such a way that the adsorbent characterization is consistent with the thermodynamic model used for equilibrium calculations.

EQUATION OF STATE AND EQUILIBRIUM CONDITION

During the past few years, we have developed extensions of cubic equations of state for confined fluids in different geometries[25,30] based on the Generalized van der Waals Theory.[35] The key results are expressions for the Helmholtz energy as a function of temperature, volume, and component amounts, from which expressions for all other thermodynamic properties can be derived. Herein, we follow the methodology reported previously. For more details, the reader is referred to our earlier papers. The chemical potential is particularly relevant to the goal of this work because of its use to determine the adsorption equilibrium condition. The chemical potential of a pure substance confined in a porous medium, for the extended Peng−Robinson EOS, is

$$\mu = \mu_0 + RT\left(\ln\left(\frac{N_{av}\lambda^3}{v-b_p}\right) + \frac{b_p}{v-b_p}\right) - F_{pr}N_{av}\varepsilon_p - \frac{a_p}{b_p}\left(\frac{\sqrt{2}}{4}\ln\left(\frac{v+(1+\sqrt{2})b_p}{v+(1-\sqrt{2})b_p}\right) + \frac{vb_p}{v(v+b_p)+b_p(v-b_p)}\right) + \left(1-(\theta+1)\frac{b_p}{v}\right)\left(1-\frac{b_p}{v}\right)^{\theta-1}(1-F_{pr})\left(RT\left(1-\exp\left(-\frac{N_{av}\varepsilon_p}{RT}\right)\right) - N_{av}\varepsilon_p\right) \quad (1)$$

where R is the ideal gas constant, T is the absolute temperature, v is the molar volume, N_{av} is Avogadro's number, ε_p is the square-well depth of the molecule-wall interaction potential, a_p and b_p are the energy parameter and volume parameter modified by confinement, respectively, F_{pr} is the fraction of fluid molecules interacting with the pore wall for random distribution of the fluid, θ is a function of the confinement geometry, λ is the de Broglie wavelength, and μ_0 is the reference chemical potential, which is related to the internal partition function.[25]

Parameter b_p is expressed in terms of the close-packing density of the fluid in the porous medium (ρ_{max}), a function of the pore geometry, by

$$b_p = \frac{N_{av}}{\rho_{max}} \quad (2)$$

Similarly, a_p is related to the confinement geometry:

$$a_p = a(T)h(r_p) \quad (3)$$

where a is the energy parameter of the Peng−Robinson EOS and h is a function of the pore radius (r_p). Following our approach for the confinement in spherical pores, the geometry-dependent terms (F_{pr}, θ, ρ_{max}, and h) can be expressed as functions of the pore radius, molecular diameter (σ), molecule-wall interaction range (δ_p), and universal parameters (c_k, A, U, B, M, ν, η, φ) as follows:

$$\begin{aligned} F_{pr} &= \frac{(r_p-\sigma/2)^3-(r_p-\sigma/2-\delta_p)^3}{(r_p-\sigma/2)^3}, \\ \theta &= \frac{r_p}{\delta_p+\sigma/2}, \\ \rho_{max}\sigma^3 &= c_1 - c_2\exp\left(c_3\left(\frac{1}{2}-\frac{r_p}{\sigma}\right)\right) + c_4\exp\left(c_5\left(\frac{1}{2}-\frac{r_p}{\sigma}\right)\right), \\ h &= \frac{A}{10} + \frac{10-A}{10(1+U\exp(-B(r_p/\sigma-M)))1/\nu} - \frac{\exp(-(r_p/\sigma/-\eta)^2/2\varphi^2)}{10\sqrt{2\pi}\varphi} \end{aligned} \quad (4)$$

The values of the parameters presented in equation 4 can be found in the work of Barbosa et al.[30] It is worth noting that this model is consistent with the bulk limit: when the pore radius grows indefinitely ($r_p \to \infty$), the original Peng−Robinson EOS[34] is recovered.

Thus, given the textural properties of the porous medium (r_p), and as long as we know the molecule-wall interaction parameters (ε_p and δ_p), the model can be used to determine the thermodynamic properties. In particular, the equilibrium condition can be expressed in terms of the equality of chemical potentials in the adsorbed phase (μ_a) and bulk phase (μ_b), which is characterized by the bulk pressure P_b and temperature T,

$$\mu_a(T, \rho_a, r_p, \varepsilon_p, \delta_p) = \mu_b(T, P_b) \quad (5)$$

This equation is the basis for the calculation of the density adsorbed on porous media (ρ_a). In this work, we solve equation 5 by using the Topliss et al.[36] method, as extended by Travalloni et al.[25]

PORE SIZE DISTRIBUTION

The theoretical basis of the thermodynamic model presented in the previous section requires prior knowledge of the pore size of the solid. However, some porous materials, such as ZIFs, have flexible structures and pore sizes that fluctuate around an average value. Thus, the ZIF's structural behavior can be better described using a PSD function. In particular, for structurally heterogeneous solids, our model can be used either for the PSD characterization or for incorporating a previously fitted PSD into the thermodynamic modeling.

For a given porous medium characterized by a PSD, the total adsorbed amount can be obtained by[33]

DOI: 10.1021/acs.iecr.9b05221
Ind. Eng. Chem. Res. 2019, 58, 19702−19708

$$n_a(T, P_b) = \int_{r_{p,min}}^{r_{p,max}} PSD(r_p)\rho_a(T, P_b, r_p)\, dr_p \quad (6)$$

where $r_{p,min}$ and $r_{p,max}$ are the lower and upper limits of the PSD, respectively, and ρ_a is the adsorbed density inside a pore whose characteristic size is between r_p and $r_p + dr_p$. To estimate the PSD, the adsorbed density for each pore was obtained by using the thermodynamic equilibrium condition (equation 5). In addition, we assume the PSD function is described by

$$PSD(r_p) = \frac{\omega}{r_p\sqrt{2\pi}} \sum_{k=1}^{NP} \frac{1}{\tau_k} \exp\left[-\frac{(\ln r_p - \nu_k)^2}{2\tau_k^2}\right] \quad (7)$$

which consists of a combination of log-normal distributions.[37] In eq 7, ω, τ_k, and ν_k are the PSD parameters and NP is the number of peaks in the PSD. From a PSD, the specific pore volume and the mean pore size, respectively, can be obtained by

$$V_p = \int_{r_{p,min}}^{r_{p,max}} PSD(r_p)\, dr_p,$$
$$\bar{r}_p = \frac{1}{V_p}\int_{r_{p,min}}^{r_{p,max}} PSD(r_p) r_p\, dr_p \quad (8)$$

Two types of parameters have to be fitted: those related to the adsorbed fluid, which are characteristic of how the fluid molecules and the pore wall interact, and those related to the PSD. The latter, in principle, represents an intrinsic feature of the adsorbent. However, because of the framework flexibility, they may also depend on the adsorbed fluid. The adopted strategy was to choose a given component and use its experimental data to fit both the PSD parameters (ω, τ_k, and ν_k) and the molecule-wall interaction parameters (ε_p and δ_p) of this component. Then, using the fitted values of the PSD parameters, specific molecule-wall interaction parameters were fitted using the experimental data for the other gases. Numerically, the integration range of equation 6 was discretized in equally spaced points, and the integral was performed by the trapezoid method. As an optimization technique, the particle swarm method[38] was adopted, making use of the least-squares objective function:

$$F = \sum_{k=1}^{N_{exp}} (n_a^k - n_{a,exp}^k)^2 \quad (9)$$

where N_{exp} is the number of experimental points, n_a^k is the adsorbed amount obtained from the equations 5 and 6, and $n_{a,exp}^k$ is the adsorbed amount experimentally measured.

RESULTS

Adsorption experimental data reported in the literature[1,12,39,40] for different ZIFs were used to infer the PSDs, based on the previously discussed EOS. Table 1 shows the model parameters as well as the average pore size and specific pore volume, and Table 2 shows the PSD parameters obtained here.

The model fitting to the adsorption data of hydrogen, oxygen, methane, ethane, propane, carbon dioxide, and propylene in ZIF-8 at 308.15 K,[1] together with the obtained PSD, is shown in Figure 1. For this adsorbent, we used the experimental data of propane in the PSD fitting. In general, the model fits the experimental data very well. In addition, the PSD obtained for ZIF-8 is markedly unimodal, with a narrow distribution around an average pore radius of 0.561 nm, which is remarkably close to the largest cavity radius of 0.57 nm reported in the literature.[41] The agreement between the specific pore volume fitted in this work (0.648 cm^3/g) and that of the computationally optimized structure reported by First and Floudas[41] (0.485 cm^3/g) is not as good. However, it is in close agreement with the value obtained by the *t*-plot method (0.65 cm^3/g).[42]

Figure 2 shows the experimental data of adsorption of carbon dioxide and methane measured by Bae et al.[39] on two different samples of mixed-ligand, Zn-based MOFs (1-M′ and 1-C′) at 298 K, along with the model fit. For both porous materials, the carbon dioxide data were used to fit the PSD. Again, very good model correlations can be observed with similar unimodal PSDs in the microporous region, although the specific pore volume is considerably different for the solids. In particular, we point out that the volume difference between the two solids solids (approximately 0.3 cm^3/g) is in qualitative agreement with the result reported by Bae et al.[39] Nonetheless, the pore volume values for the solids differ considerably from those reported by these authors using the Dubinin–Radushkevich equation ($V_p^{1-C'}$ = 0.34 cm^3/g and $V_p^{1-M'}$ = 0.064 cm^3/g).

The adsorption data of ethane, propane, and *n*-butane in ZIF-8 over a range of temperature, obtained by Pimentel and Lively,[12] were used to evaluate structural changes in the solid due to the adsorption of different gases. Initially, proceeding analogously to the previous systems, the PSD fitting was made using the butane experimental data. However, the obtained

Table 1. Model Parameters Estimated from Pure Fluid Adsorption Data and Textural Properties

adsorbent	r_p (nm)	V_p (cm^3/g)	adsorbate	ε_p/k (K)	δ_p (nm)
ZIF-8	0.561	0.648	H_2	512.34	0.012
			O_2	398.68	0.900
			CH_4	756.39	0.140
			C_2H_6	1364.38	0.158
			C_3H_8	1781.02	0.574
			CO_2	1004.30	0.144
			C_3H_6	1790.81	0.208
ZIF 1-C′	0.750	0.547	CO_2	1679.53	0.065
			CH_4	1009.08	0.100
ZIF 1-M′	0.770	0.238	CO_2	2056.64	0.093
			CH_4	1098.26	0.159
ZIF-8	0.500	0.603	C_2H_6	1341.18	0.271
	0.566	0.600	C_3H_8	1857.00	0.274
	0.656	0.600	C_4H_{10}	2215.26	0.300
ZIF-7	1.016	0.105	N_2O	1399.42	0.608
	1.016	0.102	CO_2	1318.05	0.717

Table 2. PSD Parameters Estimated from Pure Fluid Adsorption Data

adsorbent	adsorbate	$\omega \times 10^6$	ν	τ
ZIF-8	–	0.648	−21.322	0.202
ZIF 1-C′	–	0.547	−21.030	0.199
ZIF 1-M′	–	0.238	−20.998	0.174
ZIF-8	C_2H_6	0.603	−21.439	0.200
	C_3H_8	0.600	−21.332	0.230
	C_4H_{10}	0.600	−21.190	0.300
ZIF-7	N_2O	0.105	−20.710	0.072
	CO_2	0.102	−20.720	0.041

DOI: 10.1021/acs.iecr.9b05221
Ind. Eng. Chem. Res. 2019, 58, 19702−19708

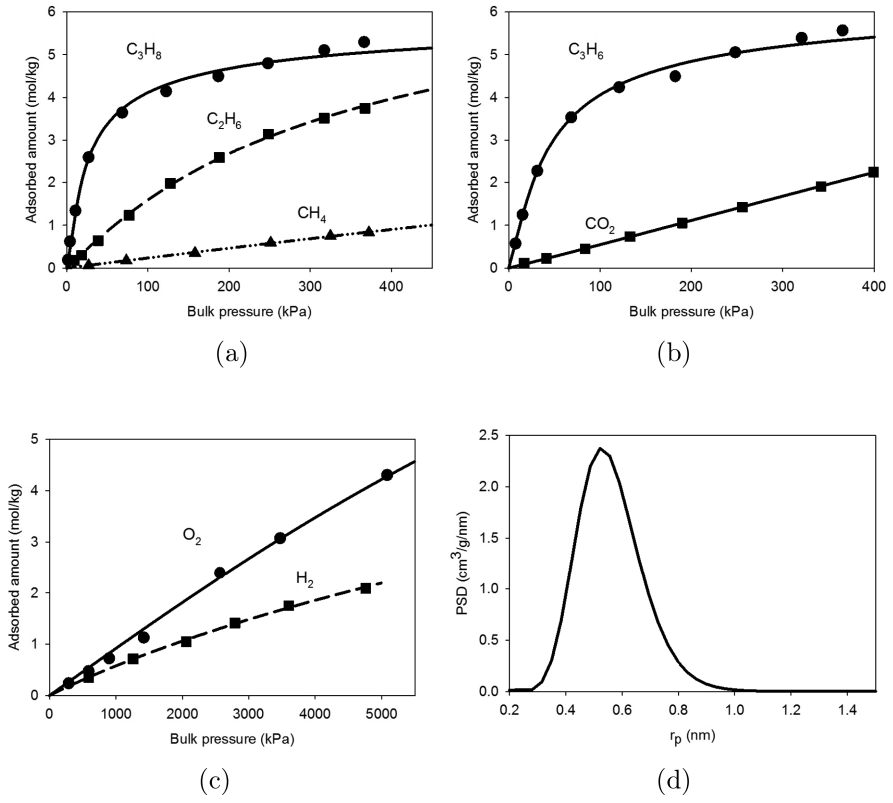

Figure 1. (a–c) Pure fluids adsorption on ZIF-8 at 308.15 K. Symbols represent the experimental data reported by Zhang et al.[1] and the lines represent the model fit. (d) Adsorbent PSD inferred from the model.

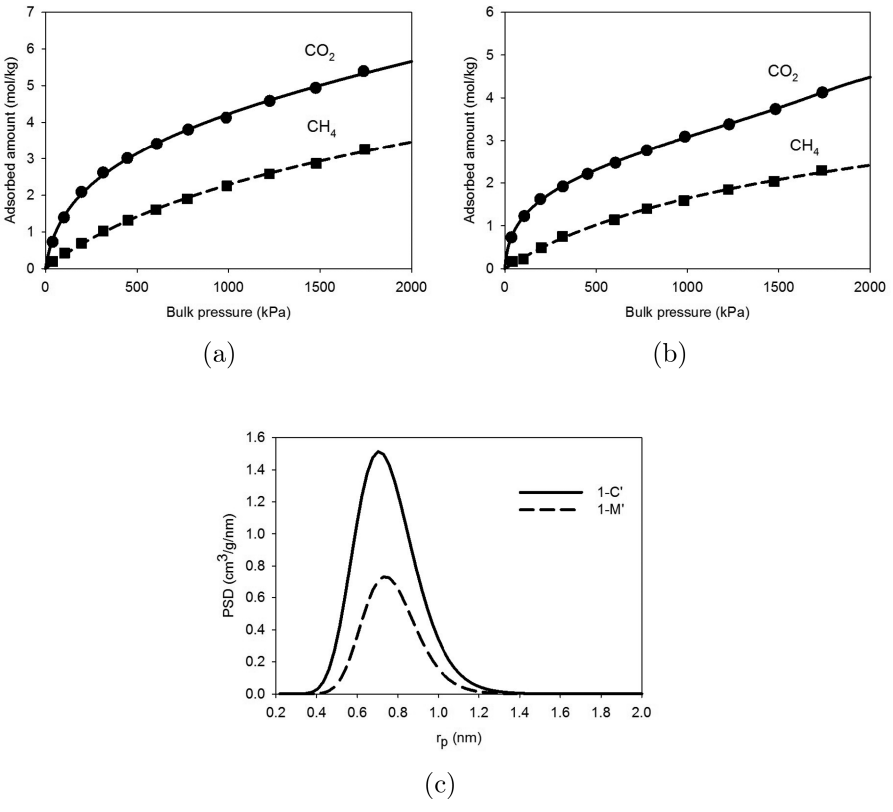

Figure 2. Carbon dioxide and methane adsorption data on two different MOFs (which are called (a) 1-C′ and (b) 1-M′) at 296.0 K. Symbols represent the experimental data reported by Bae et al.,[39] and the lines represent the model fit. (c) Adsorbent PSD inferred by the model.

DOI: 10.1021/acs.iecr.9b05221
Ind. Eng. Chem. Res. 2019, 58, 19702–19708

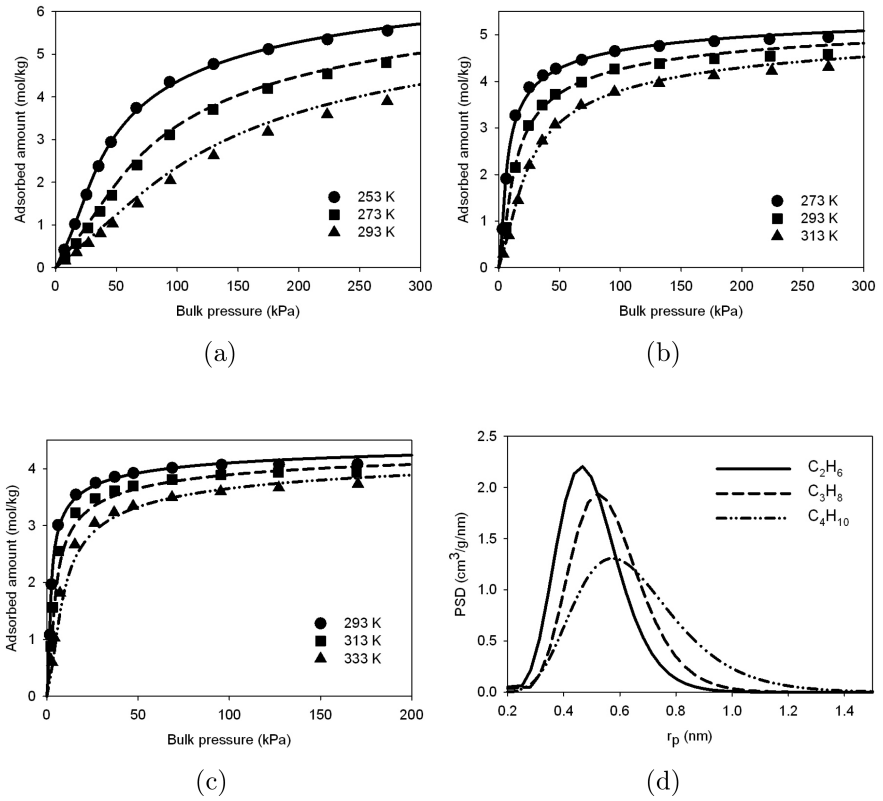

Figure 3. (a) Ethane, (b) propane, and (c) *n*-butane adsorption on ZIF-8 over a range of temperature. Symbols represent the experimental data reported by Pimentel and Lively,[12] and the lines represent the model fit at the lowest temperature and predictions at the highest temperatures. (d) Adsorbent PSD inferred by the model.

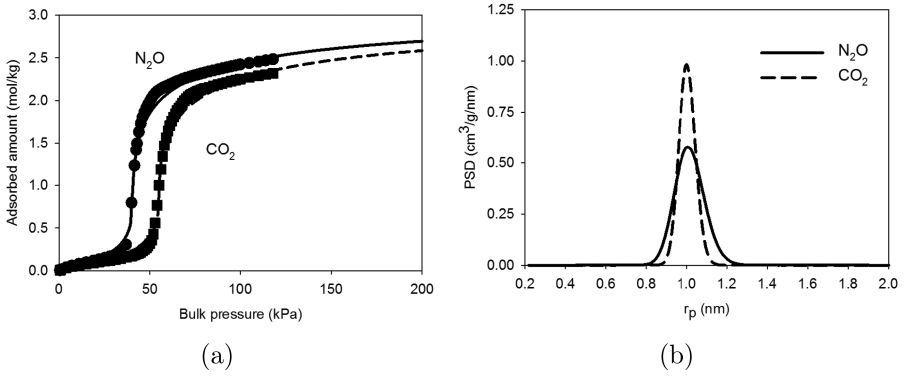

Figure 4. (a) Nitrous oxide and carbon dioxide adsorption data on ZIF-7 at 298.0 K. Symbols represent the experimental data reported by Chen et al.,[40] and the lines represent the model fit. (b) Adsorbent PSD inferred by the model.

PSD did not provide a satisfactory fit of the experimental data of the other adsorbates. Thus, PSD adjustments were made for each component at the lowest available temperature, i.e., 253 K for ethane, 273 K for propane, and 293 K for butane. Additionally, predictions were made to higher temperatures for each species. As can be seen in Figure 3, the three PSDs are unimodal, presenting almost the same specific pore volume for all species, reported in Table 1, which is in close agreement with the value reported by Peralta et al.[42] However, the average pore radii depend on the adsorbate, increasing with the growth of the molecular size. This result is in qualitative agreement with the molecular simulations of Krokidas et al.[8] and the crystallographic data of Hobday et al.,[43] which indicate that structural size parameters depend on the type of fluid molecule. This shows that our approach can correlate structural changes in the porous material due to the presence of different adsorbates. Moreover, it is possible to observe that the model satisfactorily predicted the adsorption isotherms at temperatures higher than that used for model fitting.

The final case deals with the adsorption of nitrous oxide and carbon dioxide on ZIF-7. This ZIF is known to have a flexible structure, with a gate of about 0.2 nm in diameter under vacuum[41,44] that can more than double in the presence of fluid molecules.[44] Figure 4 shows the adsorbed amount of nitrous oxide and carbon dioxide on ZIF-7 at 296.0 K[40] and the obtained PSDs. Again, different PSDs were adjusted for each chemical species, in order to verify structural changes resulting from the adsorption of each one. The specific pore volumes, equal to 0.105 cm^3/g for N_2O and 0.102 cm^3/g for CO_2, are in good agreement with the value of 0.0904 cm^3/g reported by

DOI: 10.1021/acs.iecr.9b05221
Ind. Eng. Chem. Res. 2019, 58, 19702−19708

Shahrak et al.[45] These specific pore volumes differ from the value of 0.176 cm^3/g reported by First and Floudas.[41] The fitted pore radius, equal to 1.016 nm, is larger than the largest cavity radius of 0.28 nm reported by First and Floudas[41] and the median pore radius of 0.2103 nm reported by Shahrak et al.[45] As can be observed in Figure 4, the model was able to successfully correlate the relatively complex adsorption data, which are classified as a type V isotherm.[46] This was accomplished by fitting a unimodal PSD in the micromesopore range to account for the presence of each adsorbate, obtaining similar specific pore volumes and average pore sizes. It is observed that the PSD inferred from the CO_2 adsorption data is remarkably narrower than that obtained with the N_2O data, but there is no information in the literature for comparison.

CONCLUSIONS

The Peng−Robinson equation extended to confinement in spherical cavities was used in this work to infer textural properties of some metal organic frameworks. The inclusion of the pore size distribution allowed the model to successfully correlate several adsorption isotherms. The PSDs fitted to pure fluid adsorption data were in good agreement with molecular simulation and experimental results.

Interestingly, despite the use of a general formulation that allowed the fitting of multimodal PSDs, the PSDs fitted in this work turned out to be unimodal. Besides, despite its simplicity, the adopted procedure was able to reproduce structural changes of the porous materials due to the adsorption of different chemical species, in line with literature results. This suggests that our modeling approach captured two key aspects: the regularity of the solid structure and the pore size fluctuation. In particular, we showed that the inclusion of a unimodal PSD made it possible to accurately correlate relatively complex, type V adsorption isotherms.

AUTHOR INFORMATION

Corresponding Author

*E-mail: gdbarbosa@eq ufrj.br.

ORCID

Frederico W. Tavares: 0000-0001-8108-1719

Marcelo Castier: 0000-0003-1005-1517

Notes

The authors declare no competing financial interest.

ACKNOWLEDGMENTS

We thank Drs. R. P. Lively, R. Krishna, and their co-workers for kindly providing their experimental data in tabular form. We acknowledge the financial support of CNPq, CAPES, ANP, and Petrobras (Brazil). The participation of M. Castier in this work was made possible by Grant NPRP 8-1648-2-688 from the Qatar National Research Fund (a member of Qatar Foundation). The statements made herein are solely the responsibility of the authors.

REFERENCES

(1) Zhang, C.; Lively, R. P.; Zhang, K.; Johnson, J. R.; Karvan, O.; Koros, W. J. Unexpected molecular sieving properties of zeolitic imidazolate framework-8. *J. Phys. Chem. Lett.* **2012**, *3*, 2130−2134.

(2) Kwon, H. T.; Jeong, H.-K. In Situ Synthesis of Thin Zeolitic−Imidazolate Framework ZIF-8 Membranes Exhibiting Exceptionally High Propylene/Propane Separation. *J. Am. Chem. Soc.* **2013**, *135*, 10763−10768.

(3) Kwon, H. T.; Jeong, H.-K. Highly propylene-selective supported zeolite-imidazolate framework (ZIF-8) membranes synthesized by rapid microwave-assisted seeding and secondary growth. *Chem. Commun.* **2013**, *49*, 3854−3856.

(4) Kwon, H. T.; Jeong, H.-K. Improving propylene/propane separation performance of Zeolitic-Imidazolate framework ZIF-8 Membranes. *Chem. Eng. Sci.* **2015**, *124*, 20−26.

(5) Krokidas, P.; Castier, M.; Moncho, S.; Brothers, E.; Economou, I. G. Molecular Simulation Studies of the Diffusion of Methane, Ethane, Propane and Propylene in ZIF-8. *J. Phys. Chem. C* **2015**, *119*, 27028−27037.

(6) Krokidas, P.; Castier, M.; Moncho, S.; Sredojevic, D.; Brothers, E.; Kwon, H.; Jeong, H.-K.; Lee, J.; Economou, I. ZIF-67 framework: a promising new candidate for propylene/propane separations - Experimental data and molecular simulations. *J. Phys. Chem. C* **2016**, *120*, 8116−8124.

(7) Krokidas, P.; Castier, M.; Economou, I. G. Computational Study of ZIF-8 and ZIF-67 Performance for Separation of Gas Mixtures. *J. Phys. Chem. C* **2017**, *121*, 17999−18011.

(8) Krokidas, P.; Moncho, S.; Brothers, E. N.; Castier, M.; Economou, I. G. Tailoring the gas separation efficiency of metal organic framework ZIF-8 through metal substitution: a computational study. *Phys. Chem. Chem. Phys.* **2018**, *20*, 4879−4892.

(9) Krokidas, P.; Moncho, S.; Brothers, E. N.; Castier, M.; Jeong, H.-K.; Economou, I. G. On the efficient separation of gas mixtures with the mixed linker zeolitic-imidazolate framework-7−8. *ACS Appl. Mater. Interfaces* **2018**, *10*, 39631−39644.

(10) Liu, D.; Ma, X.; Xi, H.; Lin, J. Gas transport properties and propylene/propane separation characteristics of ZIF-8 membranes. *J. Membr. Sci.* **2014**, *451*, 85−93.

(11) Hara, N.; Yoshimune, M.; Negishi, H.; Haraya, K.; Hara, S.; Yamaguchi, T. Diffusive separation of propylene/propane with ZIF-8 membranes. *J. Membr. Sci.* **2014**, *450*, 215−223.

(12) Pimentel, B. R.; Lively, R. P. Enabling kinetic light hydrocarbon separation via crystal size engineering of ZIF-8. *Ind. Eng. Chem. Res.* **2016**, *55*, 12467−12476.

(13) Gücüyener, C.; van den Bergh, J.; Gascon, J.; Kapteijn, F. Ethane/Ethene Separation Turned on Its Head: Selective Ethane Adsorption on the Metal-Organic Framework ZIF-7 through a Gate-Opening Mechanism. *J. Am. Chem. Soc.* **2010**, *132*, 17704−17706.

(14) van den Bergh, J.; Gücüyener, C.; Pidko, E. A.; Hensen, E. J.; Gascon, J.; Kapteijn, F. Understanding the anomalous alkane selectivity of ZIF-7 in the separation of light alkane/alkene mixtures. *Chem. - Eur. J.* **2011**, *17*, 8832−8840.

(15) Fairen-Jimenez, D.; Moggach, S.; Wharmby, M.; Wright, P.; Parsons, S.; Duren, T. Opening the gate: framework flexibility in ZIF-8 explored by experiments and simulations. *J. Am. Chem. Soc.* **2011**, *133*, 8900−8902.

(16) Casco, M. E.; Cheng, Y.; Daemen, L.; Fairen-Jimenez, D.; Ramos-Fernández, E. V.; Ramírez-Cuesta, A. J.; Silvestre-Albero, J. Gate-opening effect in ZIF-8: the first experimental proof using inelastic neutron scattering. *Chem. Commun.* **2016**, *52*, 3639−3642.

(17) Chokbunpiam, T.; Fritzsche, S.; Chmelik, C.; Caro, J.; Janke, W.; Hannongbua, S. Gate opening effect for carbon dioxide in ZIF-8 by molecular dynamics−Confirmed, but at high CO2 pressure. *Chem. Phys. Lett.* **2016**, *648*, 178−181.

(18) Cimino, R. T.; Kowalczyk, P.; Ravikovitch, P. I.; Neimark, A. V. Determination of isosteric heat of adsorption by quenched solid density functional theory. *Langmuir* **2017**, *33*, 1769−1779.

(19) Grégoire, D.; Malheiro, C.; Miqueu, C. Estimation of adsorption-induced pore pressure and confinement in a nanoscopic slit pore by a density functional theory. *Continuum Mech. Thermodyn.* **2018**, *30*, 347−363.

(20) Pang, Y.; Soliman, M. Y.; Sheng, J. Investigating gas-adsorption, stress-dependence, and non-Darcy-flow effects on gas storage and transfer in nanopores by use of Simplified Local Density Model. *SPE Reservoir Evaluation & Engineering* **2018**, *21*, 073−095.

(21) Chen, M.; Kang, Y.; Zhang, T.; Li, X.; Wu, K.; Chen, Z. Methane adsorption behavior on shale matrix at in-situ pressure and

DOI: 10.1021/acs.iecr.9b05221
Ind. Eng. Chem. Res. 2019, 58, 19702−19708

temperature conditions: Measurement and modeling. *Fuel* **2018**, *228*, 39−49.
(22) Schoen, M.; Diestler, D. J. Analytical treatment of a simple fluid adsorbed in a slit-pore. *J. Chem. Phys.* **1998**, *109*, 5596−5606.
(23) Zarragoicoechea, G. J.; Kuz, V. A. van der Waals equation of state for a fluid in a nanopore. *Phys. Rev. E: Stat. Phys., Plasmas, Fluids, Relat. Interdiscip. Top.* **2002**, *65*, 021110.
(24) Giaya, A.; Thompson, R. W. Water confined in cylindrical micropores. *J. Chem. Phys.* **2002**, *117*, 3464−3475.
(25) Travalloni, L.; Castier, M.; Tavares, F. W.; Sandler, S. I. Thermodynamic modeling of confined fluids using an extension of the generalized van der Waals theory. *Chem. Eng. Sci.* **2010**, *65*, 3088−3099.
(26) Travalloni, L.; Castier, M.; Tavares, F. W.; Sandler, S. I. Critical behavior of pure confined fluids from an extension of the van der Waals equation of state. *J. Supercrit. Fluids* **2010**, *55*, 455−461.
(27) Travalloni, L.; Castier, M.; Tavares, F. W. Phase equilibrium of fluids confined in porous media from an extended Peng-Robinson equation of state. *Fluid Phase Equilib.* **2014**, *362*, 335−341.
(28) Dong, X.; Liu, H.; Hou, J.; Wu, K.; Chen, Z. Phase equilibria of confined fluids in nanopores of tight and shale rocks considering the effect of capillary pressure and adsorption film. *Ind. Eng. Chem. Res.* **2016**, *55*, 798−811.
(29) Barbosa, G. D.; Travalloni, L.; Castier, M.; Tavares, F. W. Extending an equation of state to confined fluids with basis on molecular simulations. *Chem. Eng. Sci.* **2016**, *153*, 212−220.
(30) Barbosa, G. D.; D'Lima, M. L.; Daghash, S. M.; Castier, M.; Tavares, F. W.; Travalloni, L. Cubic equations of state extended to confined fluids: New mixing rules and extension to spherical pores. *Chem. Eng. Sci.* **2018**, *184*, 52−61.
(31) Tan, S. P.; Piri, M. Equation-of-state modeling of confined-fluid phase equilibria in nanopores. *Fluid Phase Equilib.* **2015**, *393*, 48−63.
(32) Franco, L. F. M.; Economou, I. G.; Castier, M. A statistical mechanical model for adsorption coupled with SAFT-VR Mie equation of state. *Langmuir* **2017**, *33*, 11291−11298.
(33) Barbosa, G. D.; Travalloni, L.; Castier, M.; Tavares, F. W. Pore size distributions from extended Peng-Robinson equations of state for fluids confined in cylindrical and slit pores. *Fluid Phase Equilib.* **2019**, *493*, 67−77.
(34) Peng, D.-Y.; Robinson, D. B. A New Two-Constant Equation of State. *Ind. Eng. Chem. Fundam.* **1976**, *15*, 59−64.
(35) Sandler, S. I. The generalized van der waals partition function. I. basic theory. *Fluid Phase Equilib.* **1985**, *19*, 238−257.
(36) Topliss, R. J.; Dimitrelis, D.; Prausnitz, J. M. Computational aspects of a non-cubic equation of state for phase-equilibrium calculations. Effect of density-dependent mixing rules. *Comput. Chem. Eng.* **1988**, *12*, 483−489.
(37) Jin, Z.; Firoozabadi, A. Thermodynamic modeling of phase behavior in shale media. *SPE Journal* **2016**, *21*, 190−207.
(38) Schwaab, M.; Biscaia, J. C., Jr.; Monteiro, J. L.; Pinto, J. C. Nonlinear parameter estimation through particle swarm optimization. *Chem. Eng. Sci.* **2008**, *63*, 1542−1552.
(39) Bae, Y.-S.; Mulfort, K. L.; Frost, H.; Ryan, P.; Punnathanam, S.; Broadbelt, L. J.; Hupp, J. T.; Snurr, R. Q. Separation of CO_2 from CH_4 using mixed-ligand metal-organic frameworks. *Langmuir* **2008**, *24*, 8592−8598.
(40) Chen, D.-L.; Wang, N.; Wang, F.-F.; Xie, J.; Zhong, Y.; Zhu, W.; Johnson, J. K.; Krishna, R. Utilizing the gate-opening mechanism in ZIF-7 for adsorption discrimination between N_2O and CO_2. *J. Phys. Chem. C* **2014**, *118*, 17831−17837.
(41) First, E. L.; Floudas, C. A. MOFomics: Computational pore characterization of metal-organic frameworks. *Microporous Mesoporous Mater.* **2013**, *165*, 32−39.
(42) Peralta, D.; Chaplais, G.; Simon-Masseron, A.; Barthelet, K.; Pirngruber, G. D. Separation of C6 paraffins using zeolitic imidazolate frameworks: comparison with zeolite 5A. *Ind. Eng. Chem. Res.* **2012**, *51*, 4692−4702.
(43) Hobday, C.; Woodall, C.; Lennox, M.; Frost, M.; Kamenev, K.; Düren, T.; Morrison, C.; Moggach, S. Understanding the adsorption process in ZIF-8 using high pressure crystallography and computational modelling. *Nat. Commun.* **2018**, *9*, 1429.
(44) Arami-Niya, A.; Birkett, G.; Zhu, Z.; Rufford, T. E. Gate opening effect of zeolitic imidazolate framework ZIF-7 for adsorption of CH4 and CO2 from N2. *J. Mater. Chem. A* **2017**, *5*, 21389−21399.
(45) Niknam Shahrak, M.; Niknam Shahrak, M.; Shahsavand, A.; Khazeni, N.; Wu, X.; Deng, S. Synthesis, gas adsorption and reliable pore size estimation of zeolitic imidazolate framework-7 using CO2 and water adsorption. *Chin. J. Chem. Eng.* **2017**, *25*, 595−601.
(46) Brunauer, S.; Deming, L. S.; Deming, W. E.; Teller, E. On a theory of the van der Waals adsorption of gases. *J. Am. Chem. Soc.* **1940**, *62*, 1723−1732.

DOI: 10.1021/acs.iecr.9b05221
Ind. Eng. Chem. Res. 2019, 58, 19702−19708